A New Method for Processing Impact Excited Continuous-Scan Laser Doppler Vibrometer Measurements

Matthew S. Allen[1] and Michael W. Sracic

Department of Engineering Physics

University of Wisconsin-Madison

535 Engineering Research Building

1500 Engineering Drive

Madison, WI 53706

[1]Corresponding Author: Email: msallen@engr.wisc.edu, Tel: 608-890-1619 (US), Fax: 608-263-7451 (US)

Abstract:

A scanning Laser Doppler Vibrometer (LDV) can acquire non-contact vibration measurements from a structure with high spatial detail in an automated manner; one only need redirect the laser via computer controlled mirrors to acquire measurements at additional points. However, since most LDV systems are only capable of measuring one point at a time, conventional scanning LDV cannot be effectively employed in some situations, for example when the time record is long at each measurement point or when the structure changes with time. Conventional scanning LDV systems are also difficult to employ with impact excitation because there is considerable variation in the impact location, angle and the character of the impacts, which leads to errors in the mode shapes that are extracted from the measurements. This paper presents a method by which one can determine the mode shapes, natural frequencies and damping ratios of a structure from as little as one response record by sweeping the laser continuously over the vibrating structure as the measurement is acquired. This work presents a novel resampling approach that transforms the continuous-scan measurements into pseudo-frequency response functions, so they can be processed using standard identification routines to find the modal parameters of the structure. Specifically, this work employs a standard multi-input-multi-output

identification routine and the complex mode indicator function to the Continuous-Scan Laser Doppler Vibrometry (CSLDV) measurements. The method makes no assumptions regarding the shape or properties of the surface and only requires that the laser scan periodically and that the structure vibrate freely. The method is demonstrated experimentally on a free-free beam, identifying the first nine mode shapes of the beam at hundreds of points from a few time histories. For this system, this represents a two-order of magnitude reduction in the time needed to acquire measurements with the LDV.

1. Introduction

Laser Doppler Vibrometers (LDV) provide the unique ability to measure the vibration of a surface without having to attach a transducer that might locally stiffen or mass-load the structure. They have been widely employed to measure vibration on small, lightweight structures such as hard disk drive heads, microstructures [1-3], other systems that might be modified by attaching traditional contact transducers, and also on rotating systems where contact transducers cannot easily be attached [4]. Scanning LDV systems include computer controlled mirrors so one can control the position of the laser spot on the structure automatically and with high spatial accuracy, and align the measurement points with images of the structure. In the past decade, they have also found increasing use in the automotive and aerospace areas, where the structures are not as sensitive to mass loading, but the vibrometer is still attractive because it allows one to acquire measurements at a large number of spatial points in an automated manner.

One significant drawback of conventional scanning laser Doppler Vibrometer systems is that they only measure the response at one point at a time. (Efforts are underway to develop systems with an array of lasers [5], but it is difficult to reduce the cost per laser of high performance LDV systems.) All commercially available systems direct the laser at a point on the test structure and acquire a measurement over a time window that is long enough to allow the structure's impulse response to decay. Then the laser is directed to a new point on the structure and the process is repeated. Typically, several measurements are acquired at each location to reduce the effects of noise. If the structure has lightly damped modes and the natural frequencies of those modes are low, then each response may be quite long, and the total test time may be prohibitive. This is true whether transient or persistent excitation is

employed if conventional frequency response estimation techniques are utilized. Because of the length and nature of these tests, electromagnetic shakers are usually used to excite the test structure, but this contacting exciter may modify the structure, which is often precisely what one was trying to avoid by selecting a non-contact measurement device. Automated excitation devices can also be time-consuming to set up and may require special fixturing, both of which increase the cost of the test.

Recently, a different measurement approach has been proposed where the laser is swept continuously over the surface of the structure as a measurement is acquired. The response measured by a sweeping laser does not have the same mathematical form as a standard impulse or frequency response, so specialized methods must be developed to process them. Sriram *et al.* appear to have been the first to suggest this in the early 1990's [6-8], and they did successfully extract at least one mode from a small beam. More recently, Stanbridge, Martarelli and Ewins began investigating a similar concept, coining the term Continuous-Scan Laser Doppler Vibrometry (CSLDV). They developed two methods that derive the operating deflection shape of a structure from the measured CLSDV response, both of which require that the test object exhibit purely sinusoidal motion. The first derives a polynomial series representation of the operating deflection shape from the amplitudes of harmonics in the response [9-11], and the second demodulates the signal to obtain the ODS at many points directly [12]. Because a single excitation frequency is used, the process must typically be repeated at a number of frequencies to obtain all of the modes of interest; efforts are still underway to develop methods that treat modes with close natural frequencies [13]. On the other hand, when single-frequency excitation is practical, fast sine-fit methods can be used to obtain spatially dense measurements of ODSs quickly, and this approach has already been implemented into commercial SLDV systems. Vanlanduit et al. have also explored CSLDV, combining multi-sine excitation and CSLDV to estimate broadband FRFs and a Fourier Series description of the mode shapes [14]; as with the single-sine methods, one must typically employ an electromagnetic shaker or some other contacting excitation device to obtain a suitable multi-sine input.

Stanbridge, Martarelli and Ewins also instigated the use of CSLDV with impact excitation in [15, 16]. Their approach relates the amplitudes of peaks in the spectrum of an impulse response to coefficients in the polynomial series expansion that they used in [9-11]. They have obtained accurate, smooth mode shapes using their method, whereas conventional roving hammer tests give jagged mode

shapes because the angle of the hammer blows and the point at which the hammer strikes are difficult to control precisely [17]. Some disadvantages of their method are that it requires specialized algorithms to process the CSLDV measurements and is limited to situations where the structure has lightly damped modes with large natural frequencies relative to the laser scan speed.

This work presents a new CSLDV method that is effective for structures with low natural frequencies; these are the structures that require the longest measurement times using traditional scanning LDV. The key to the approach is the way in which the mode shapes are extracted from the measurements; the methods presented here exploit algorithms that were recently developed to identify the parameters of Linear Time-Periodic (LTP) systems [18-20]. When applied to CSLDV, these methods essentially decompose the free response measurement into a set of frequency response functions that would have been measured by a stationary sensor at each point traversed by the laser, so the collection of responses can be processed using standard procedures for Linear Time-Invariant (LTI) systems. The resulting mode shapes capture the motion of the structure at hundreds of points along the scan path, so the density of the information obtained is hundreds of times higher than would be obtained by conventional LDV in the same amount of time, and is limited only by the noise in the signal and the sample rate of the LDV. One can also add data from additional input locations in much the same way one does for time invariant systems, so the method is easy to expand to multi-input-multi-output (MIMO) testing situations, and important tools such as the Mode Indicator Function [21] can be directly applied to detect modes with close natural frequencies. There are also some potential advantages with regards to laser speckle noise because this method collects all of the speckle noise to a single frequency line.

This paper proceeds as follows. Section 2 presents the new analysis method and compares it to existing techniques. The method is applied to identify the modes of a free-free beam in Section 3, with particular emphasis on elucidating the effect of the laser scan frequency. Conclusions are presented in Section 4.

2. Theory

The response of a freely vibrating, linear time-invariant structure with underdamped modes can be expressed as a sum of decaying exponentials in terms of the modal parameters of the structure. Each

mode shape of the structure, $\phi_r(\mathbf{x})$, depends on the point at which the laser vibrometer is directed and its orientation, which shall be denoted with the vector $\mathbf{x}$, so the response can be written as,

$$y(t) = \sum_{r=1}^{2N} \phi_r(\mathbf{x}) C_r e^{\lambda_r t}$$
$$\lambda_r = -\zeta_r \omega_r + i\omega_r \sqrt{1-\zeta_r^2} \ , \ \lambda_{r+N} = -\zeta_r \omega_r - i\omega_r \sqrt{1-\zeta_r^2} \quad (1)$$

where λ_r is the rth complex eigenvalue, which is expressed in terms of the rth natural frequency, ω_r, and damping ratio, ζ_r. The constant C_r is the complex amplitude of mode r, which depends upon the structure's initial conditions or on the impulse used to excite the structure.

If the laser traverses a known, periodic path $\mathbf{x}(t) = \mathbf{x}(t+T_A)$ with period T_A or scan frequency $\omega_A = 2\pi/T_A$, one can write eq. (1) as.

$$y(t) = \sum_{r=1}^{2N} \phi_r(t) C_r e^{\lambda_r t}$$
$$\phi_r(\mathbf{x}(t)) = \phi_r(t) = \phi_r(t+T_A) \quad (2)$$

This is identical to the expression for the free response of a Linear Time Periodic (LTP) system given in [20], so the methods used there can be applied to identify the modal parameters $\phi(t)_r$ and λ_r. The following sections briefly review the two methods presented in [20], elaborating on some points that are important to CSLDV. This work focuses on the first method, dubbed the lifting method (also called the Multiple Discrete Time Systems (MDTS) method in a preliminary work [18, 19]). The second method in [20], based on Fourier Series Expansion (FSE), is similar to the approach employed by Stanbridge, Martarelli and Ewins, as will be discussed in Section 2.2.

2.1. Lifting Method

The lifting method eliminates the time dependence of the mode shapes, $\phi(\mathbf{x}(t))$, by sampling the response only at instants in which $\mathbf{x}(t)$, is equal to a finite set of values $\mathbf{x}(t_i) = \mathbf{x}_i$. Typically the sample increment is much smaller than the scan period, so setting the sampling increment at $\Delta t = T_A/N_A$ where N_A is an integer, one obtains samples at N_A points along the scan path. Current LDV systems are capable of sampling at rates of MHz or higher, thousands of times faster than current scan rates, so thousands of

pseudo-points $\mathbf{x}_i$ can potentially be acquired in one CSLDV test. The signal is then separated into N_A sequences y^*_k, each defined by,

$$y^*_k = y\left(k\Delta t + mT_A\right) \quad m = 0,1,...,N_c - 1 \tag{3}$$

where N_c denotes the number of cycles of the scan period that are acquired. Impulse sampling is assumed, so this is a "starred" signal (see, for example, [22] pp. 75-76 for a discussion of sampling and starred signals).

This collection of free responses is the same as what would be measured by an array of sensors that were fixed to the points $\mathbf{x}_i$, except that the responses are not measured simultaneously; the kth response is delayed from the first $k\Delta t$. Writing eq. (2) for each of the m instants, $m = 0, \ldots, N_c\text{-}1$, that are captured in the kth sequence, we obtain the following.

$$y^*_k = \sum_{r=1}^{2N}\left(\phi_r\left(k\Delta t\right)C_r e^{\lambda_r(k\Delta t)}\right)e^{\lambda_r(mT_A)}. \tag{4}$$

This is a superposition of exponentials, and the coefficient of each exponential is constant (for any particular k), so each of these responses has the same mathematical form as the response of a linear state space system (the coefficient or residue may be complex even if the system has real modes). We collect the responses for all k and define the lifted response $y^{*L} = [y^*_0, y^*_1, \ldots y^*_{NA\text{-}1}]^{\mathrm{T}}$, which one can now see has the following mathematical form

$$y^{*L}\left(mT_A\right) = \sum_{r=1}^{2N} A_r e^{\lambda_r\left(mT_A\right)} \quad m = 0,...,N_c - 1, \tag{5}$$

where the residue, A_r, of the lifted system is

$$A_r = C_r\left[\left(\phi_r\left(0\right)e^{\lambda_r(0)}\right) \quad \cdots \quad \left(\phi_r\left((N_A - 1)\Delta t\right)e^{\lambda_r\left((N_A-1)\Delta t\right)}\right)\right]^T. \tag{6}$$

This shows that the lifted response, y^{*L}, has the same form as the impulse response of a state space (arbitrarily damped) LTI system, so one can apply virtually any standard, state-space identification routine

to it to identify the eigenvalues λ_r and residues A_r of the system. Equation (6) can then be used to find $\phi_r(\mathbf{x}(t))$ from A_r, up to a scale factor C_r.

It is important to note that the sample increment of the lifted responses is T_A, so if any of the modes of the system has a natural frequency larger than $\omega_{max} = \omega_A/2$, then that mode will be aliased in the lifted response. Ideally, one would avoid this issue by choosing the mirror scan frequency to be at least twice the highest natural frequency that is excited. This is not always possible because the scan frequency is limited by the mirror dynamics and perhaps by speckle noise considerations [11, 23]. If a mode is aliased, its true (unaliased) natural frequency must be determined in order to find its mode shape using eq. (6). If the system is proportionally damped so that $\phi_r(\mathbf{x}(t))$ is approximately real, then a simple approach can be used. The authors have observed that one tends to find a highly complex mode shape $\phi_r(\mathbf{x}(t))$ if an aliased eigenvalue is used to extract the mode shape, $\phi_r(t)$, from A_r in eq. (6) In this work, we have identified the unaliased eigenvalues by applying the following procedure for each mode:

1.) Construct $(\lambda_{test})_{r,k} = \lambda_r + ik\omega_A$ over some appropriate range of k spanning the range of aliasing that is expected. For the tests described here, k= -25…25 was used.

2.) Use each $(\lambda_{test})_{r,k}$ to extract the mode shape, $(\phi_{test})_{r,k}(t)$, from A_r in eq. (6).

3.) Determine which test mode, $(\phi_{test})_{r,k}(t)$, has the best modal phase co-linearity. Then, the corresponding eigenvalue $(\lambda_{test})_{r,k}$ is the true (unaliased) eigenvalue, and the unaliased natural frequency can be computed by taking its absolute value.

Using this approach, accurate mode shapes have been obtained even when a mode's frequency was an order of magnitude larger than the scan frequency, as demonstrated in Section 3, or when modes were aliased such that they had close frequencies in the lifted measurements. Even if two modes are aliased to exactly the same frequency, they may still be distinguishable if they have different damping, but it is preferable to choose a scan frequency to avoid this scenario if possible because the mode shapes of two modes with the same frequency can be difficult to separate. If the two modes are not distinguishable, then their shapes will not be correct and the unaliasing approach would probably fail. Fortunately, if this occurs then one can always supplement the CSLDV measurements with measurements at other scan frequencies or with conventional, stationary point LDV measurements to locate each of the natural frequencies.

It is often desirable to use a frequency domain approach to identify the modal parameters λ_r and A_r from a set of measurements. The lifted response, y^{*L}, is convenient to process in the frequency domain, but the aliasing that is possible with CSLDV measurements complicates the issue, so the extension to frequency domain identification will be reviewed briefly here. One approach is to take the z transform of eq. (5), yielding

$$Z\left\{y^{*L}\right\} = \sum_{r=1}^{2N} \frac{zA_r}{z - e^{\lambda_r T_A}}. \tag{7}$$

The Discrete Fourier Transform (DFT or FFT) of the time sequence y^{*L} is approximately equal to its z transform with $z = e^{i\omega T_A}$, so long as the time sequence is sufficiently small at the end of the time record (see [24]). Hence, one can take $\mathrm{DFT}\{y^{*L}\} \approx \mathrm{Z}\{y^{*L}\}$ and fit the measured response to the pole-residue description in eq. (7). Many algorithms are available for doing this, most of which use linear least squares to fit the response to a ratio of polynomials in z (see, for example, [25]).

Alternatively, one can develop a continuous time approach by relating the z domain response to the Laplace transform using the following relation (see [22] p. 87),

$$Z\left\{y^{*L}\right\}\Big|_{z=e^{i\omega T_A}} = Y^{*L}(i\omega) = \frac{1}{T_A}\sum_{k=-\infty}^{\infty} Y^{L}(i\omega + i\omega_A k) \tag{8}$$

where $Y^{L}(i\omega)$ and $Y^{*L}(i\omega)$ are the Laplace transforms of $y^{L}(t)$ and y^{*L} respectively and

$$Y^{L}(i\omega) = \sum_{r=1}^{2N} \frac{A_r}{i\omega - \lambda_r}, \tag{9}$$

Equation (8) reveals that one needs an infinite sum of continuous-time modes to approximate the DFT of y^{*L}. However, each modal contribution falls off at frequencies far from $\omega = |\lambda_r|$, so if each mode has decayed to a negligible level at the edges of the frequency band, then the response is well approximated with 2N continuous time modes and one can apply a continuous-time modal parameter identification routine to y^{*L} to find the modal parameters λ_r and A_r. On the other hand, if a mode falls near $\omega = 0$ or $\omega = \omega_A/2$, then its tail aliases back into the frequency band and one must add additional modes to the

response to accurately fit the measurements. This relationship between the z and Laplace domain descriptions has been observed in other works, for example by [26], who used z domain polynomials to fit a continuous-time model simply because they improve the numerical conditioning of the identification algorithm.

The Discrete Fourier Transform (DFT or FFT) of y^{*L} is here dubbed a pseudo-Frequency Response Function (pFRF), the term "pseudo" being used because the residues in eqs. (4-6), although related to the mode shapes, differ from the usual definition, so the pseudo-FRFs do not have all of the properties of conventional FRFs. However, they do share some very important properties. For example, consider a case where a structure has two frequencies that are very close. If the force that initiated the free vibration is repeated at a different location, then the constants C_r for each mode change, changing the shape of the response observed in the vicinity of the close natural frequencies. Hence, the set of responses can be treated as an additional column of the pseudo-FRF matrix, the corresponding residue matrices are rank one, and concepts such as the Mode Indicator Function [21] and multi-input multi-output identification [25, 27-29] can be used. The primary advantage of the lifting procedure is that it makes it possible to directly apply all of these powerful tools to extract the modes of a structure from CSLDV measurements.

2.2. Fourier Series Expansion Method (FSE)

One can gain additional insight into the CSLDV process by examining the spectrum of the measured CSLDV signal (eq. (2)). Because the scan pattern $\mathbf{x}(t)$ is periodic, the mode shapes can be expanded into a Fourier Series as follows,

$$C_r \phi_r(t) = \sum_{m=-N_B}^{N_B} B_{r,m} \, \mathrm{e}^{(im\omega_A t)} \tag{10}$$

where it is assumed that only the coefficients from $-N_B$ to $+N_B$ are significant. Substituting into eq. (2) and moving the summations to the outside results in the following.

$$y(t) = \sum_{r=1}^{2N} \sum_{m=-N_B}^{N_B} B_{r,m} \, \mathrm{e}^{\left((\lambda_r + im\omega_A)(t-t_0)\right)} \tag{11}$$

This is mathematically equivalent to the impulse response of an LTI system with $2N(2N_B + 1)$ eigenvalues

$$\lambda_{FSE,r,m} = \lambda_r + im\omega_A \tag{12}$$

The amplitude of the response of each of these apparent modes is determined by $B_{r,m}$, the mth Fourier coefficient of the rth mode shape. Hence, the bandwidth of a CSLDV signal is governed by both the natural frequencies $|\lambda_r|$ of the excited modes and the number of terms required to represent their mode shapes in a Fourier series.

Stanbridge and his associates utilized a similar representation to identify the modes of a cantilever beam from transient CSLDV responses [16], although they represent the mode shape with a power series so non-periodic scan patterns can be used. They then employ modal analysis to identify each of the coefficients $B_{r,m}$ and use those to approximate a power series model for the mode shape. One difficulty associated with this approach is that there may be many, many peaks in the CSLDV spectrum (see Figures 4 and 5, which are discussed later). This necessitates a customized modal parameter identification algorithm to fit the response at each collection of eigenvalues $\lambda_{FSE,r}$. Another alternative is to use a standard LTI identification algorithm and then post process the resulting eigenvalues to determine which of the identified eigenvalues correspond to each $\lambda_{FSE,r}$, although such an approach necessitates the use of high order matrix polynomials [21] which brings additional computational cost and increases ill conditioning. Furthermore, the collection of identified eigenvalues is unlikely to obey the relationship in eq. (12) precisely, leading to inaccuracies and user frustration. On the other hand, the lifting approach augments the number of outputs, but the model order remains the same. A large number of spatial points are easily accommodated using, for example, the modal parameter identification methods in [25, 27, 30]. Allen has processed thousands of frequency response functions simultaneously using the algorithm in [27].

2.3. Noise and resolution limitations of CSLDV

In principle, one could obtain data from millions of pseudo-points over the surface of a structure from a single sweep of the laser spot if one could sample quickly enough. In practice, the actual resolution that can be obtained is limited by measurement noise. The dominant noise source in CSLDV

measurements will most likely be laser speckle noise, which occurs because the laser spot is moving in plane relative to the surface. Noise effects must be considered in order to design a successful CSLDV system, but the impact of speckle noise on laser vibrometer measurements has only recently begun to be appreciated [4, 31, 32]. Fortunately, it has been observed that speckle noise is predominantly periodic, occurring at the scan frequency and its multiples [11], so one can often choose the scan frequency such that the dominant speckle noise frequencies are distinct from the frequencies that carry the response of the system. This is easiest to visualize with the lifting method, because it aliases all of the speckle noise to the zero frequency line, so if the modal density is relatively low, then one can usually adjust the scan frequency so that none of the modes are aliased to near zero frequency, and then the speckle noise can be easily ignored. There is also a non-periodic component to the speckle noise that limits the accuracy of the measurements, but it has not been studied extensively; the authors are currently exploring these issues [23].

3. Experimental Application

The proposed continuous scan vibrometry method was evaluated by applying it to an aluminum (Al 6061 T6) beam with dimensions 971.6 by 25.4 by 6.35 millimeters. The beam is light and flexible, and hence it might be modified by attaching contact transducers or excitation devices, so CSLDV is attractive. The beam was suspended by 2.38mm diameter bungee cords during the test to simulate a free-free condition, as shown in Figures 1 and 2. The support system was designed so that the rigid body modes would have natural frequencies about ten times lower than the first elastic mode, [33], while also minimizing x-directional swinging and rotation in the x,y-plane, because these rigid body motions would alter the position of the scan path on the beam.

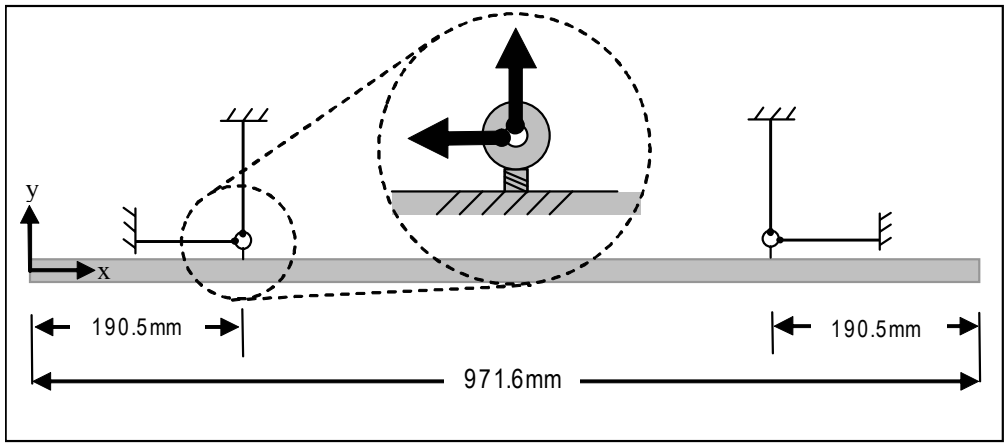

Figure 1: Schematic and dimensions of test setup.

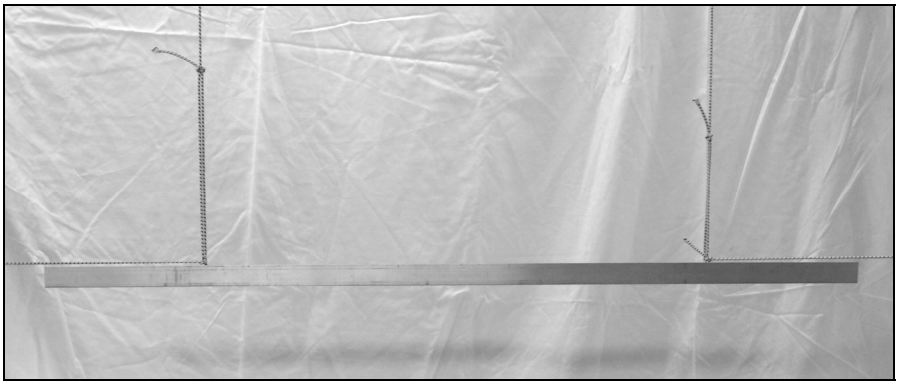

Figure 2: Photograph of aluminum beam and support system.

3.1. Hardware Setup

A schematic of the measurement hardware for the experiment is shown in Figure 3, which includes the following:

i) Polytec® PSV-400 80kHz scanning laser vibrometer

ii) Custom cable to externally control the scan-mirror servo motors

iii) Tektronix AFG 3022 Dual Channel Arbitrary Function Generator

iv) PCB Piezotronics modally tuned ICP impact hammer 086C01

A custom cable was used to replace the mirror control signal with a user-defined voltage signal generated by the function generator. Sinusoidal signals with varying frequencies were used to drive the x-direction mirror, and the signal amplitude was manually adjusted such that the laser swept the full length of the beam. The y-direction scan-capability was not utilized in this study.

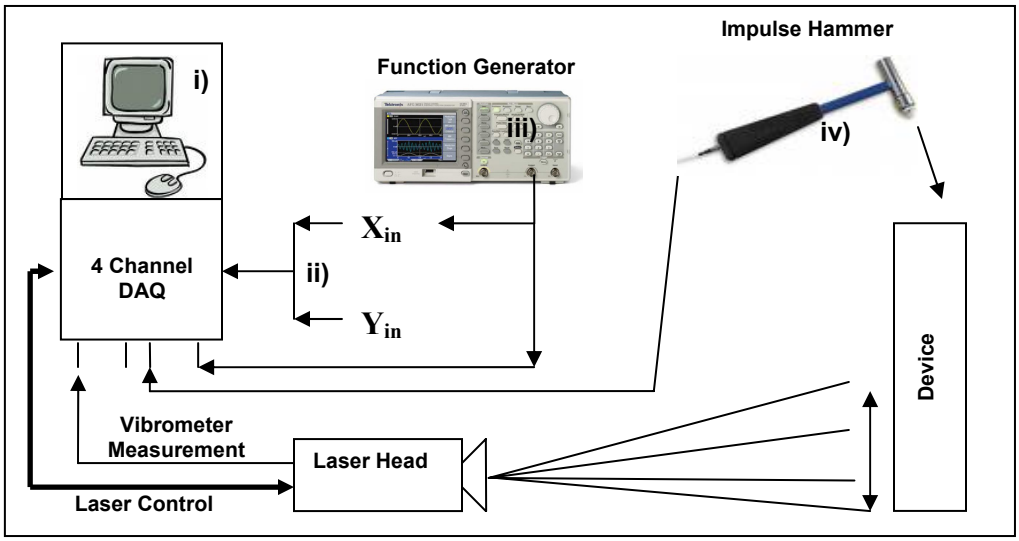

Figure 3: Schematic of Data Acquisition Hardware

The signal used to drive the mirrors was recorded by the data acquisition system along with the response, and used in post-processing to determine the location of the laser spot as a function of time. The input voltage $v(t)$ was assumed to be related to the position of the laser spot $x(t)$ by a linear dynamic system such that in the frequency domain

$$X(f_{scan}) = G(f_{scan})V(f_{scan}) \tag{13}$$

where $f_{scan} = \omega_A/(2\pi)$ is the scan speed. The magnitude and phase of $G(f_{scan})$ were determined as follows. The distance between the end of the laser path and the ends of the beam was recorded and used to determine the magnitude of the scale factor relating voltage and laser spot position. Initial tests revealed that there was also a significant phase delay between the voltage sinusoid and the x-position. This was clearly visible in the mode shapes that were identified from the CSLDV responses (shown later), because the mode shapes differed for the forward and backward sweeps of the laser. The phase delay was found by adjusting the phase of $x(t)$ relative to $v(t)$ until the mode shapes for the forward and backward sweeps agreed as closely as possible. Many mirror systems are capable of measuring the mirror angles directly, circumventing this step, but this procedure does serve to reveal the dynamic characteristics of the mirror system. Table 1 shows the gain and phase of the mirror system for each scan frequency used in this study. The large phase delay at 100 Hz suggests that we are approaching the limit of the mirror system.

f_{scan} (Hz)	Gain (mm/V)	Phase (deg)
21	360	-8.9
51	351	-21.5
100*	320	-43

Table 1: Linear gain and phase between the mirror drive signal and laser position.
**Correction factor included to account for nonlinearities in the mirror response.*

Using a 51 Hz scan frequency, the LDV vibration signal, mirror drive signal and hammer force signal were recorded for five inputs located at x-positions equal to 559 mm, 629 mm, 705 mm, 781 mm, and 857 mm with respect to the x-y coordinate system shown in Figure 1. The experiment was repeated with 21 and 100 Hz scan frequencies using the same inputs except with the input at 629 mm replaced with one at 895 mm. No attempt was made at averaging the time series or spectra to reduce noise in the LDV signal, but each mode responds to many of the inputs and the MIMO identification approach used here does identify the mode shapes globally, so one does, in effect, obtain averaged mode shapes. If further averaging were desired, additional measurements from those same inputs could also have been included in the MIMO data set. This approach is convenient unless one desires a large number of averages, in which case it would be preferable to have a spectral approach for averaging the measurements as is used in conventional modal analysis; this is a topic of current research. Data acquisition was triggered by the force hammer, and then the portions of each of the time records occurring before and during the force pulse were deleted to obtain the free-response of the beam. The sampling rate was 20.48kHz, which was adequate to capture the full bandwidth of the CSLDV signal. Thirty seconds of response data was acquired, which was the time required for the vibration signal to decay to a small level. An exponential window with a decay constant of $0.30s^{-1}$ was then applied to the vibrometer signal to reduce the effects of leakage and noise. This was approximately equal to the minimum decay constant of any of the elastic modes, which was found to be optimum in [27] when a free vibration signal is contaminated with Gaussian noise.

3.2. Experimental Results

Figures 4 and 5 show the frequency spectrum of a CSLDV measurement due to impact excitation at *x = 781 mm*, and where the scan frequency was 51 Hz, the sampling frequency was 20.48kHz and

2^19 samples were collected. The complexity of the CSLDV signal is immediately apparent from the multitude of peaks in the spectrum. Equation (11) suggests that peaks should be present near each of the modal frequencies, and at the modal frequencies plus or minus integer multiples of scan frequency. This is easiest to see in Figure 5, which shows an expanded view of the spectrum from 0 to 300 Hz. For example, the natural frequency of the 1st bending mode was found to be at 17.5 Hz, and the response shows a peak at that frequency. Peaks can also be seen at 17.5 Hz plus multiples of the scan frequency, such as 68.5 Hz and 119.5 Hz (17.5+51m Hz for m = 1 and m = 2.). Other peaks are seen due to the conjugate eigenvalue, $\mathrm{conj}(\lambda)$, of the 17.5 Hz mode, which occur at frequencies of -17.5+51m Hz = 84.5, 135.5 and 186.5 Hz). Laser speckle noise is also visible at some of the harmonics of the scan frequency, most noticeably at 51 and 102 Hz in Figure 5.

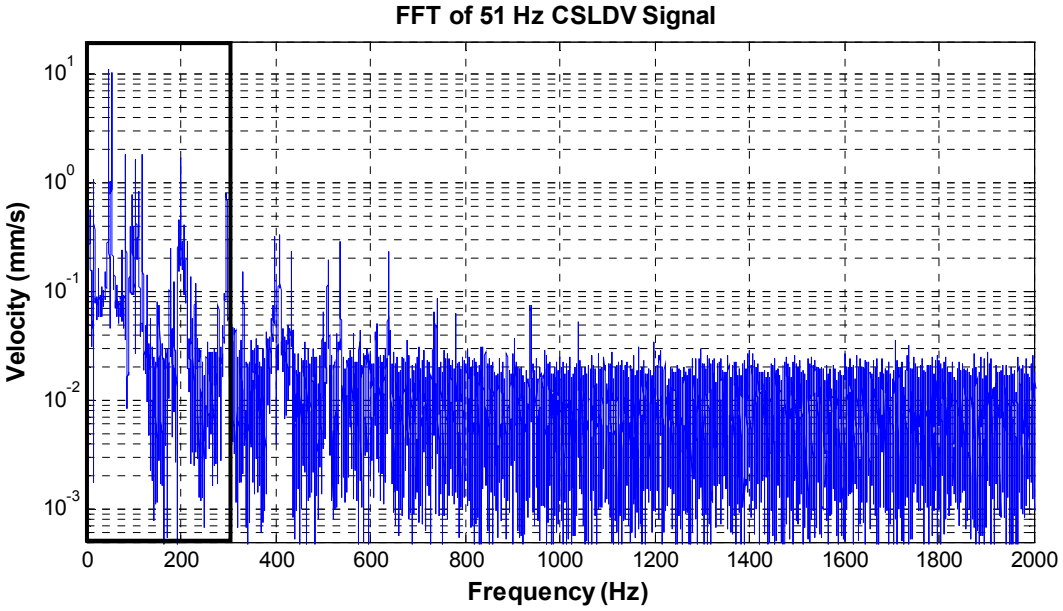

Figure 4: FFT of CSLDV signal for input at x = 781 mm

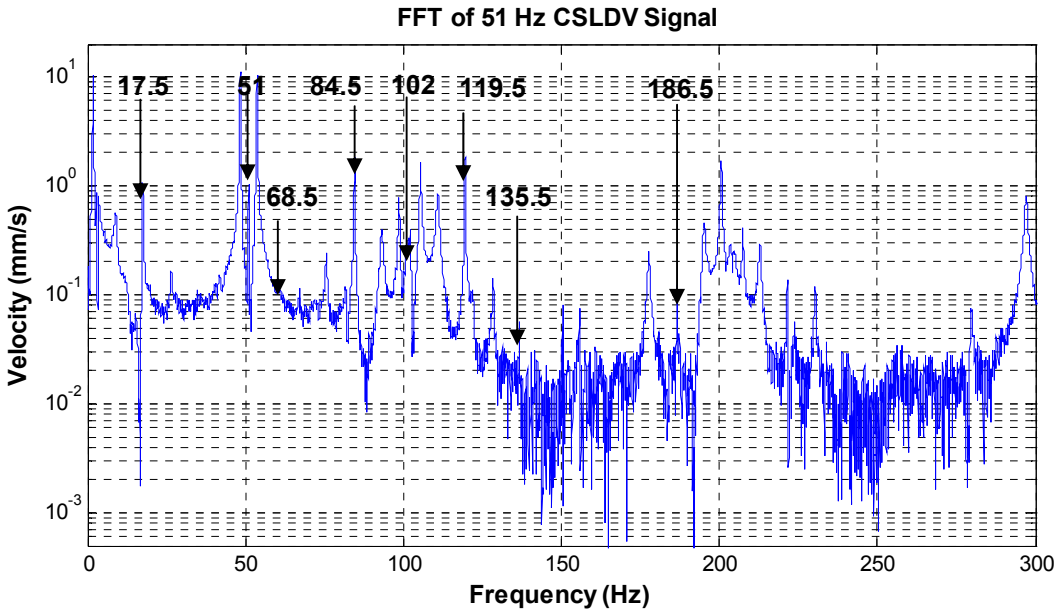

Figure 5: Expanded view of CSLDV signal in Figure 4

The measured signals were resampled to be precisely synchronous with the scan frequency, which was found to be 51.0004 Hz by fitting a sinusoid to the measured mirror drive signal. Resampling was performed simply by padding the FFT with zeros and then taking the IFFT so that the sample increment was decreased by a factor of four. Then, linear interpolation was used to obtain the response at the desired instants. The signals, corresponding to the excitation at the five drive points, were then decomposed into lifted signals and an FFT was applied resulting in a 402 response point, 5 input, 644 frequency line pseudo-FRF matrix. A beam such as this has modes with well spaced natural frequencies, but since the hammer excites modes well beyond f_{max} (25.5 Hz in this case), many of the bending modes are aliased to lower frequencies which may be close to the low frequency modes. In order to see whether aliasing causes any of these to have close frequencies in the lifted response, the complex mode indicator function (CMIF) was formed for the response set, and is shown in Figure 6.

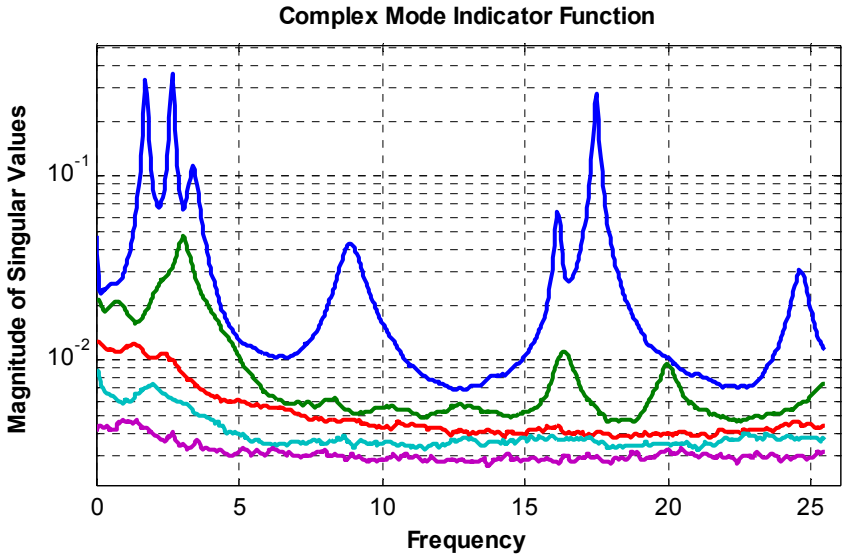

Figure 6: Complex Mode Indicator Function (CMIF) of lifted CSLDV measurements with 51 Hz scan speed and five input locations. The curves correspond to the five singular values of the pseudo-FRF matrix.

The CMIF reveals that the lifting method has resulted in a much simpler spectrum than the original CSLDV spectrum in Figures 4 and 5. The reason for this is that the harmonics corresponding to each mode, which cluttered the spectrum of the original CSLDV signal, have been folded onto one peak in the lifted responses. The CMIF essentially averages over all pseudo-points, so the result is a clean spectrum showing one peak per mode of the beam. The CMIF reveals nine modes below 25.5 Hz, seven of which give rise to peaks in the first singular value and two that appear in the second singular value at 0.9 and 20 Hz. There are a few additional peaks in the second singular value, most notably at 4 Hz and 16.5 Hz, but these are not modes but artifacts of the CMIF that occur when two modes overlap [34].

In an ideal situation, the scan frequency would be more than twice the highest natural frequency of interest, and aliasing would not occur, but the maximum scan frequency that this particular mirror system could produce was still much lower than the frequencies of many of the excited modes, so aliasing was unavoidable and scan frequencies of 21, 51, and 100 Hz were evaluated to explore its effect, using the five inputs mentioned previously. The Algorithm of Mode Isolation (AMI) [28, 30, 35, 36] was used to extract the modal parameters of the beam from each 5-input data set. The identification was performed with both z domain and Laplace domain models to see whether aliasing was important for these measurements. Figure 7 shows a composite [30] or average of the pseudo-FRFs of the velocity response for the 21 Hz scan frequency. A composite of AMI's reconstruction of the FRFs, using a z

domain model, is also shown and an additional curve shows the difference between the measurements and the z domain reconstruction. The s domain reconstruction is not shown, but the difference between it and the measurements is shown, labeled "Measured – (S fit)". The difference curve for the s-domain curve-fit is nearly twice as large as that for the z-domain, revealing that the z domain model fits the measurement more closely. A similar comparison was made for 51 and 100 Hz scan frequencies and, as expected, there was a less significant difference between the s and z domain reconstructions at those scan frequencies, presumably because aliasing is less severe.

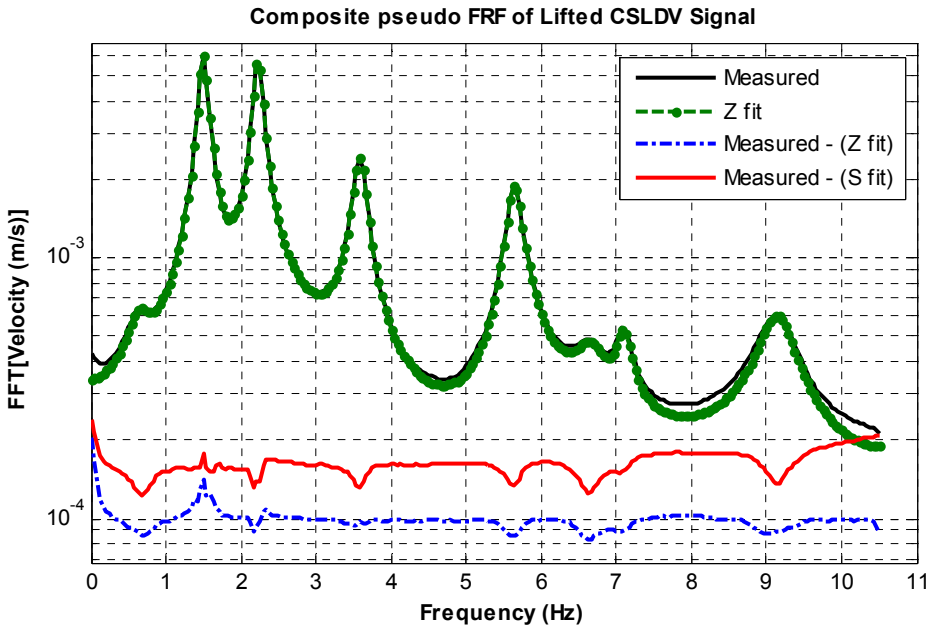

Figure 7: Composites of pseudo-FRFs for 21 Hz scan frequency, AMI reconstructions of pseudo-FRFs using z domain model and the difference between the measured and z domain reconstruction. A Laplace domain fit was also performed (not shown) and the composite of the difference between it and the measurements is also shown.

Figure 8 shows composites of the pseudo-FRFs obtained using scan frequencies of 21, 51, and 100 Hz. A 20.48 kHz sample rate was used for all of the data sets, so the 21, 51, and 100 Hz data sets had 976, 402 and 205 pseudo-points respectively after resampling. AMI identified the aliased eigenvalues of the structure and the residues at each pseudo-point. The unaliasing procedure described in Section 2.1 was automated and proved effective in identifying the true or unaliased natural frequencies of the beam from the identified eigenvalues and residues. The marker near each peak in Figure 8 gives the unaliased natural frequency of the mode that was identified at that peak, illustrating the effect that the scan-frequency has on aliasing the natural frequencies. As the scan frequency decreases, the unaliased

bandwidth decreases while the number of modes excited by the hammer remains the same, so the modal density increases. Also, aliasing decreases the imaginary part of each mode's complex eigenvalue, but the real part does not change, so the damping ratio of each aliased mode appears to increase as the scan frequency decreases. As a result, the high frequency modes become increasingly obscured by other modes as the scan frequency decreases. This is explained by the fact that the force spectrum (not shown) was observed to fall off quickly, so that at 500 Hz its power spectral density is less than a hundredth of its peak value at 20 Hz, as one might expect for impact excitation with a plastic-tipped hammer. As a result, the seventh bending mode, at 428 Hz, is the highest mode that is significantly excited, and it could not be extracted when the 21 Hz scan frequency was used.

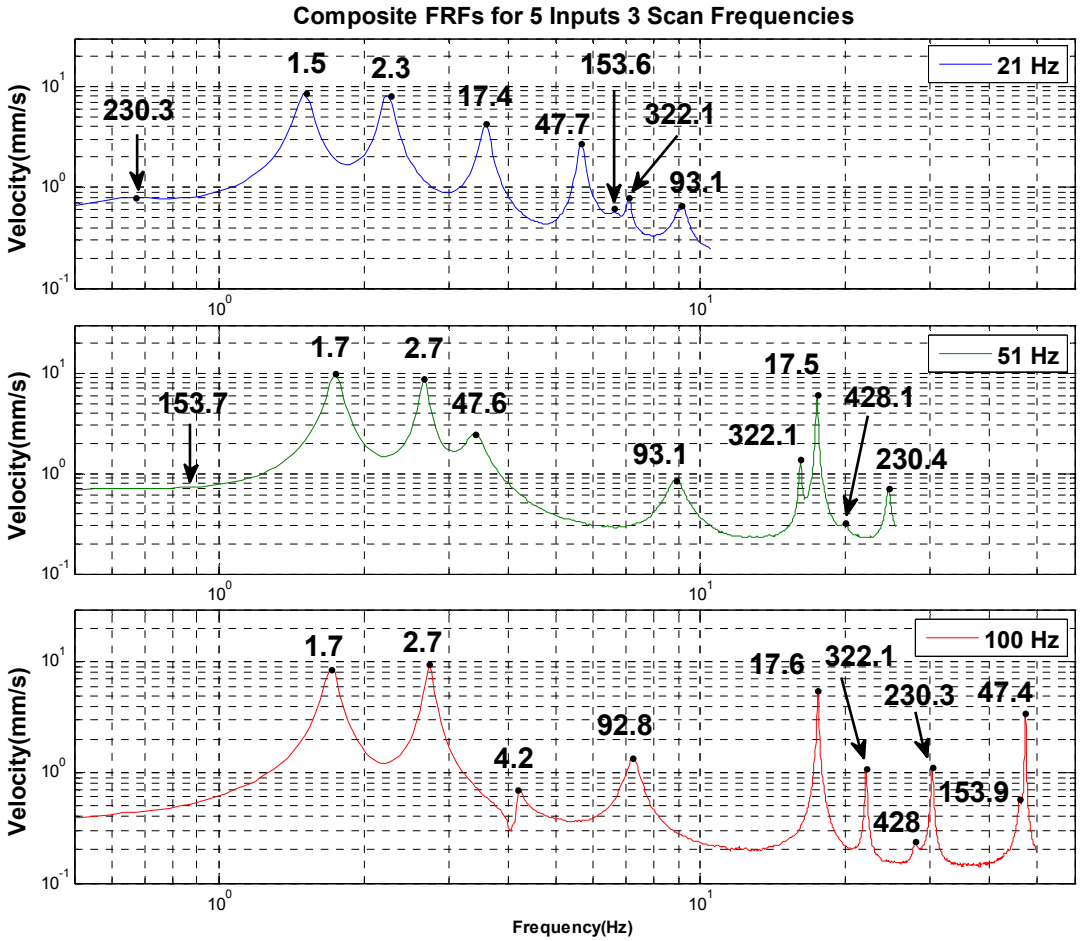

Figure 8: Composite of pseudo-FRF matrices for 21, 51 and 100 Hz scanning frequencies. Labels give the frequencies of the modes that were identified by AMI from each set of measurements.

Table 2 compares the natural frequencies and damping ratios of the modes identified from the MIMO data at each of the scan frequencies. Both the estimates of the true frequencies (Unaliased Freq), as determined from the unaliasing procedure in Section 2.1, and the frequencies at which they were identified in the lifted responses (AMI Freq) are shown. The damping ratios shown were computed from the AMI identified eigenvalues after unaliasing and after accounting for the exponential window, so they should be the same from one scan frequency to the next. The estimated natural frequencies of the bending modes differ by no more than 1% between all three data sets. The modes with unaliased frequencies less than 5 Hz are rigid body modes. Their frequencies are seen to vary somewhat between the different tests, presumably due to variation in the tension of the bungee cords used to suspend the beam. Two of the rigid body modes appear at 1.7 and 2.7 Hz in the measurements with 51 and 100 Hz scan frequencies, but in the 21 Hz measurements they appear at 1.5 and 2.3 Hz, suggesting that the bungees were not as tight in that test. The third rigid body mode at 4.2 Hz was observed only in the 100 Hz measurements. The bungee tension may also account for some of the differences between the identified bending mode frequencies, but those differences are quite small. On the other hand, there is considerable scatter in the identified damping ratios. Similar damping ratios were obtained with the identification algorithm for each data set using Laplace and z domain models, so each set of damping ratios seems to be consistent with that particular data set, but there are a few results that are suspect. For example, Figure 8 shows that the 4^{th} mode was weakly excited and aliased to frequencies where other modes were dominant, so one would expect some difficulty in accurately identifying that mode's damping.

To validate these results, a few measurements were acquired with the laser spot held stationary and using the hammer to excite the beam at a few locations. AMI was also used to identify the natural frequencies and damping ratios from this small set of measurements, and they are compared with those found using CSLDV in Table 2. The natural frequencies agree quite well with those identified by AMI, and the damping ratios are also quite similar to those found using CSLDV.

Mode #, Bending Mode #	Fixed Point		21Hz CSLDV			51 Hz CSLDV			100 Hz CSLDV		
	Freq (Hz)	Damp (%)	AMI Freq (Hz)	Unaliased Freq (Hz)	Damp (%)	AMI Freq (Hz)	Unaliased Freq (Hz)	Damp (%)	AMI Freq (Hz)	Unaliased Freq (Hz)	Damp (%)
1, -	1.73	0.86	1.50	1.50	0.86	1.74	1.74	0.97	1.71	1.71	1.02
2, -	2.65	0.47	2.22	2.22	0.57	2.67	2.67	0.52	2.74	2.74	0.50
3, 1	17.49	0.17	3.59	17.41	0.23	17.49	17.49	0.17	17.56	17.56	0.19
4, 2	47.56	0.20	5.64	47.64	0.11	3.41	47.60	0.28	47.41	47.41	0.12
5, 3	93.24	0.19	9.15	93.14	0.21	8.90	93.11	0.35	7.25	92.75	0.23
6, 4	153.7	0.14	6.64	153.6	0.11	0.54	153.5	0.16	46.10	153.90	0.17
7, 5	230.4	0.062	0.66	230.4	0.048	24.64	230.4	0.090	30.35	230.35	0.049
8, 6	322.1	0.30	7.10	322.1	0.017	16.15	322.1	0.017	22.11	322.11	0.017
9, 7	428.0	0.017	-	-	-	20.01	428.0	0.023	27.90	427.91	0.022

Table 2: Natural frequencies, unaliased and as identified, and damping ratios of CSLDV data identified by AMI for three different scan frequencies.

Figures 9 and 10 show the mode shapes obtained from the CSLDV data for the 51 and 21 Hz scanning frequencies respectively. Since the scale of the experimental mode vectors is arbitrary using this procedure, the experimental shapes shown in Figures 9 and 10 were scaled to have the same norm as the analytical ones, so only the shapes of the vectors is of interest in those plots. The experimental shapes agree very well with the analytical shapes which are shown in black, although the 4^{th} and 7^{th} bending modes (153.5 and 428 Hz) found using the 51 Hz scan frequency do show a fair amount of noise. The 4^{th} mode was situated near two dominant rigid body modes in the aliased spectrum, making it very difficult to extract. The 7^{th} mode is very weakly excited, yet with some care it was possible to extract it from the measurements. One also observes that there are a few pseudo points on the right hand side of the beam that seem to be mis-estimated in the 21Hz measurements. The reason for this is not known, but it is possible that the laser fell off of the edge of the beam for an instant during one of those tests.

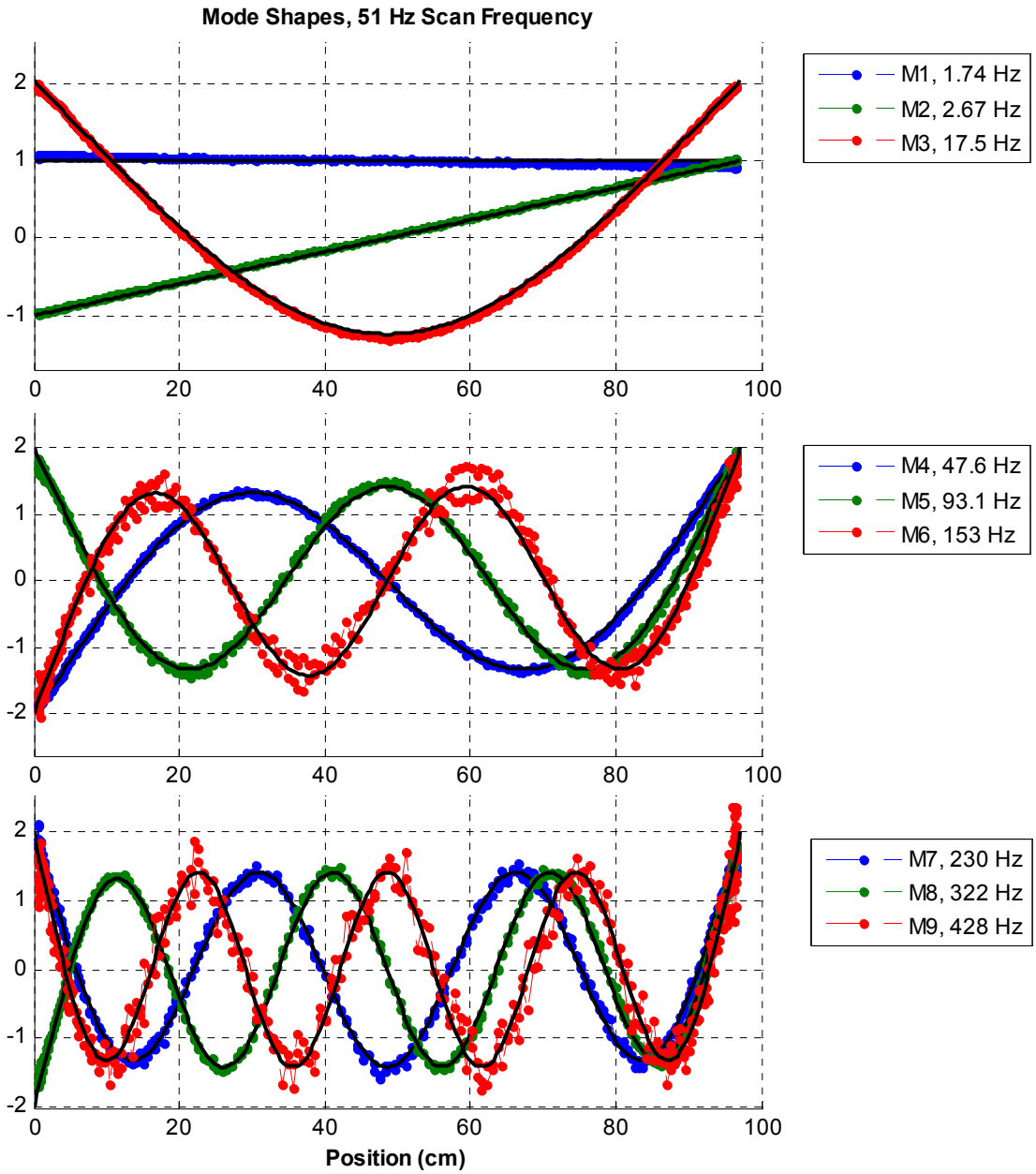

Figure 9: Mode shapes for free-free beam obtained experimentally using CSLDV with 51Hz scanning frequency, compared to analytical shapes. Solid black lines denote the analytical Euler-Bernoulli shape; dots show the experimentally obtained shapes at each pseudo-measurement point.

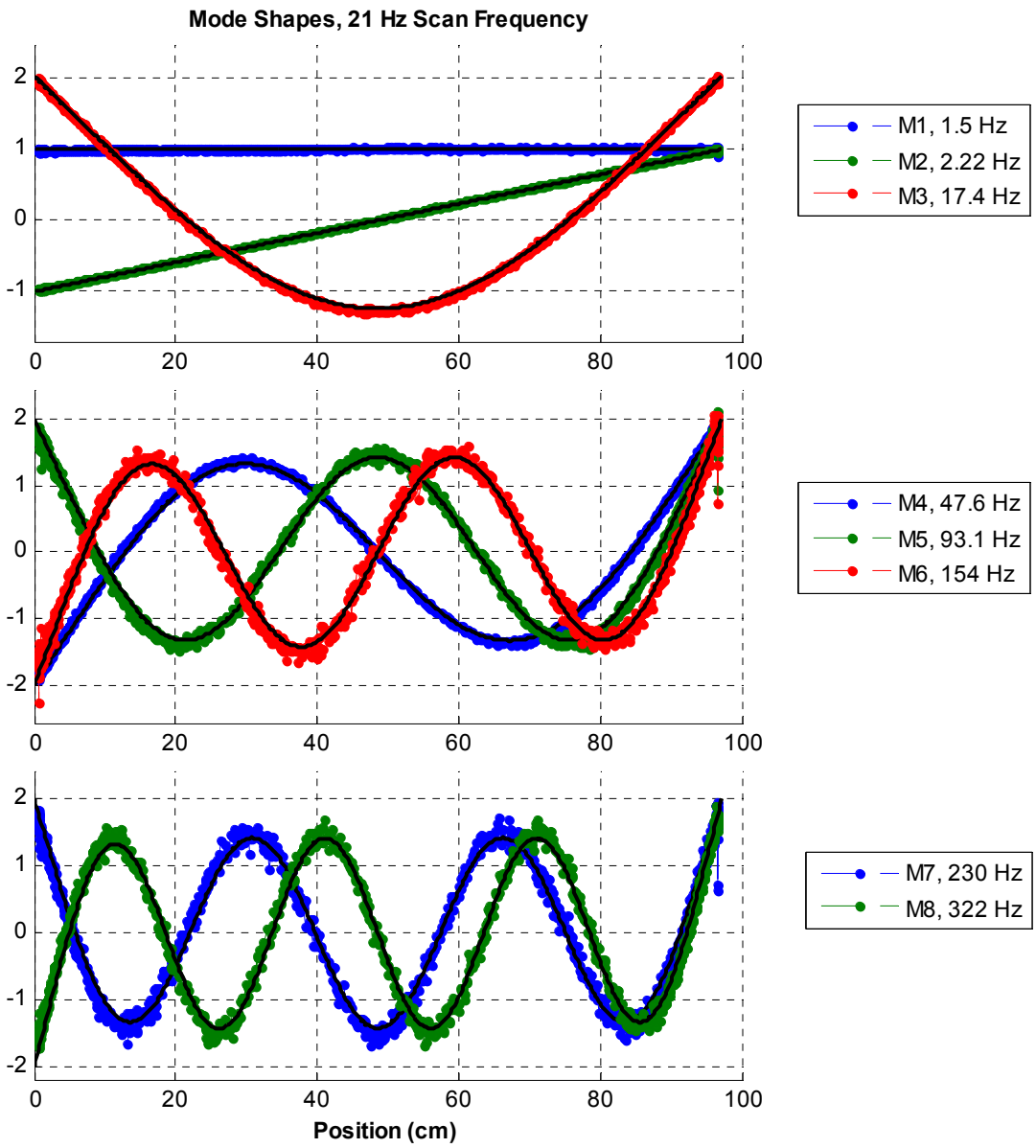

Figure 10: Mode shapes for free-free beam obtained experimentally using CSLDV with 21Hz scanning frequency, compared to analytical shapes. Solid black lines denote the analytical Euler-Bernoulli shape; dots show the experimentally obtained shapes at each pseudo-measurement point.

The Modal Assurance Criterion (MAC) values were computed between each of the identified modes and the analytical modes of a free-free Euler Bernoulli beam of the same length, and are shown in Table 3. All of the MAC values are above 0.98, except that for the 7th bending mode, which is still quite high. The MACs are shown for the modes identified using z and Laplace domain models for the 21 and 51 Hz scan frequencies. In each case, the modes identified using a z domain model almost always have slightly higher MAC values, although the difference is really only significant for the 7th bending mode. The

relationship between the mirror voltage signal and the laser spot position had to be modified slightly for the 100 Hz measurement to account for nonlinearity of the mirror response. A third harmonic term whose amplitude was about 5% of $G(f_{scan})$ was added to the transfer function in eq. 13 to account for the nonlinearity, resulting in the MAC values shown below.

Mode #, Bend. Mode #	21Hz		51 Hz		100 Hz
	z	Laplace	z	Laplace	z
1,-	0.9998	0.9997	0.9977	0.9980	0.9993
2,-	0.9999	0.9999	0.9987	0.9985	0.9989
3,1	0.9992	0.9990	0.9992	0.9990	0.9990
4,2	0.9979	0.9976	0.9993	0.9991	0.9962
5,3	0.9930	0.9821	0.9966	0.9961	0.9954
6,4	0.9863	0.9579	0.9822	0.9831	0.9927
7,5	0.9820	0.9640	0.9935	0.9902	0.9912
8,6	0.9840	0.9754	0.9956	0.9956	0.9851
9,7			0.9449	0.9017	0.9350

Table 3: Modal Assurance Criterion (MAC) values between analytical Euler-Bernoulli Modes and those identified using CSLDV. Modes were identified using both z and s (Laplace) domain models at the 21 and 51 Hz scan rates.

Discussion

For this system, very good estimates of the first eight modes (six elastic modes) are obtained using CSLDV at a variety of scan frequencies. The good agreement between the analytical and CSLDV mode shapes is surprising, especially considering the fact that no averaging was performed, but this is a relatively simple structure with good surface reflectivity. Of course, one should bear in mind that the analytical model may not be a perfect representation of the experimental structure. Unfortunately, experimental validation is not practical. As shown in [17], when using conventional scanning LDV with impact testing, one obtains mode shapes with considerable errors due to the inherent variability in the location, orientation and character of the hammer blows, so that type of test would not have the resolution needed to validate these results. One could use a shaker in conjunction with LDV to obtain better consistency, but that might modify the structure so the comparison would not be all that valuable. The support system is soft, so it should not affect the beam's natural frequencies much, but it most likely does add damping to the beam, because, as Carne and Griffith discussed, [33], a structure's apparent damping is sensitive to the support system. This might explain the discrepancy between the damping ratios for the

three scan frequencies. Modal parameter identification was repeated a number of times and the results were consistent, suggesting that the damping ratios identified were appropriate for each data set.

It is significant to note that a scan frequency of 51 Hz is nearly 20 times smaller than what would be required to avoid aliasing the 428 Hz mode; the 21 Hz scan rate is 30 times too small for the 322 Hz mode, the highest mode that was identified using that scan rate, yet good results were obtained using either of these scan frequencies. However, each of these scan frequencies aliases all of the modes to distinct frequencies. If two modes were aliased so that they land at the same frequency, the mode shapes would most likely degrade, so it seems advisable to use as high a scan frequency as possible, or to repeat the CSLDV procedure at a few scan frequencies until all of the modes can be resolved. If the scan frequency were very low compared to the natural frequencies, then aliasing might be very severe and it would not be wise to use the lifting procedure. In that case, the FSE method or the methods of Stanbridge *et al.* [16, 17] would be preferred, yet the damping must be light and the modes adequately spaced to employ those methods. To illustrate the difference, consider the following. The lowest bending mode of this system occurs at 17.5 Hz. If one must capture harmonics spanning $-10 < m < 10$, then a scan frequency of 1.75 Hz or less must be used with the FSE method so that the lower harmonics are contained between 0 and 17.5 Hz. However, at such a low scan frequency, the laser might not even traverse the length of the beam before some of the high frequency modes had vanished, so the higher modes might not be identifiable using such a low scan frequency.

It was noted that 976, 402 and 205 pseudo-points were obtained at the 21, 51 and 100 Hz scan frequencies. However, as Stanbridge *et al.* have pointed out, the actual resolution of the data is determined by the number of Fourier coefficients that are significant in the response, so the number of points in not necessarily a measure of the resolution of the measurement. On the other hand, including a surplus of measurement points may allow one to average out experimental scatter to some extent. One can relate the results of the lifting algorithm to those that would have been obtained using the FSE method by taking the FFT of the mode shapes obtained from the lifted measurements. This was done for some of the mode shapes found here, and it was observed that the mode shapes could be reproduced quite faithfully using only the Fourier coefficients for $-15 < m < 15$. The low order mode shapes required even fewer coefficients. In a keynote lecture at the 2007 International Modal Analysis Conference, Ewins

noted that this feature could be used in model updating, to more effectively quantify the amount of independent information that is available in a modal database.

4. Conclusions

This work presented a new technique that extracts the mode shapes, natural frequencies and damping ratios of a structure from Continuous Scan Laser Doppler Vibrometer measurements on freely-vibrating structures. This work has demonstrated that accurate mode shapes can be obtained along a scan path using impact excitation and CSLDV. The difference in testing time between CSLDV and the conventional approach is significant. In this work, the first nine modes (seven elastic modes) of an aluminum beam were acquired at hundreds of points from five time records totaling 2.5 minutes. Many hours of response data would be needed to achieve similar spatial resolution using conventional methods. Also, it was noted that one obtains remarkably self-consistent measurements with CSLDV because the response at each point is acquired from a single free response and using the same sensor. This might be valuable when seeking to detect defects in a structure or when updating finite element models [37].

This work presented a new processing technique for CSLDV measurements based on lifting. The primary advantage of the new technique is that it allows one to use standard modal analysis tools to extract the mode shapes from a set of CSLDV measurements. This work demonstrated the use of the complex mode indicator function and multi-input-multi-output modal parameter extraction, both of which were readily applied to the lifted CSLDV measurements. One could also apply spatial condensation [21] to reduce the number of outputs, or any of a number of other modal parameter extraction techniques. The proposed lifting method is most effective when the scan frequency is high relative to the natural frequencies of the structure, although for this particular structure most of the modes that were excited were readily extracted even when the scan frequency was more than an order of magnitude smaller than the highest frequency of interest. One must also consider the noise level when choosing a scan frequency. Fortunately, the lifting method aliases most of the laser speckle noise to the zero frequency line, so it was not observed to corrupt the measurements much. There is also a non-periodic component to the speckle noise, which the authors are currently seeking to characterize [23].

5. References

[1] H. Sumali, J. E. Massad, D. A. Czaplewski, and C. W. Dyck, "Waveform design for pulse-and-hold electrostatic actuation in MEMS," *Sensors and Actuators A (Physical),* vol. 134, pp. 213-20, 2007.

[2] M. Allen, H. Sumali, and D. Epp, "Piecewise-linear restoring force surfaces for semi-nonparametric identification of nonlinear systems," *Nonlinear Dynamics,* vol. 54, pp. 123-135, 2008.

[3] B. Ohler, "Cantilever spring constant calibration using laser Doppler vibrometry," *Review of Scientific Instruments,* vol. 78, pp. 63701-1, 2007.

[4] S. J. Rothberg, "Laser vibrometry. Pseudo-vibrations," *Journal of Sound and Vibration,* vol. 135, pp. 516-522, 1989.

[5] J. M. Kilpatrick and V. Markov, "Matrix laser vibrometer for transient modal imaging and rapid nondestructive testing," in *8th International Conference on Vibration Measurements by Laser Techniques: Advances and Applications*, Ancona, Italy, 2008, p. 709809.

[6] P. Sriram, J. I. Craig, and S. Hanagud, "Scanning laser Doppler vibrometer for modal testing," *International Journal of Analytical and Experimental Modal Analysis,* vol. 5, pp. 155-167, 1990.

[7] P. Sriram, S. Hanagud, and J. I. Craig, "Mode shape measurement using a scanning laser doppler vibrometer," *International Journal of Analytical and Experimental Modal Analysis,* vol. 7, pp. 169-178, 1992.

[8] P. Sriram, S. Hanagud, and J. I. Craig, "Mode shape measurement using a scanning laser doppler vibrometer." vol. 1 Florence, Italy: Publ by Union Coll, Schenectady, NY, USA, 1991, pp. 176-181.

[9] A. B. Stanbridge, M. Martarelli, and D. J. Ewins, "Measuring area vibration mode shapes with a continuous-scan LDV," *Measurement,* vol. 35, pp. 181-9, 2004.

[10] M. Martarelli, "Exploiting the Laser Scanning Facility for Vibration Measurements," in *Imperial College of Science, Technology & Medicine*. vol. Ph.D. London: Imperial College, 2001.

[11] M. Martarelli and D. J. Ewins, "Continuous scanning laser Doppler vibrometry and speckle noise occurrence," *Mechanical Systems and Signal Processing,* vol. 20, pp. 2277-89, 2006.

[12] C. W. Schwingshackl, A. B. Stanbridge, C. Zang, and D. J. Ewins, "Full-Field Vibration Measurement of Cylindrical Structures using a Continuous Scanning LDV Technique," in *25th International Modal Analysis Confernce (IMAC XXV)* Orlando, Florida, 2007.

[13] A. B. Stanbridge and D. J. Ewins, "Extraction of damped and undamped natural mode shapes from area-scan ODSs," in *Seventh International Conference on Vibration Measurements by Laser Techniques (AIVELA)*. vol. 6345 Ancona, Italy: International Society for Optical Engineering, Bellingham WA, WA 98227-0010, United States, 2006, p. 63450.

[14] S. Vanlanduit, P. Guillaume, and J. Schoukens, "Broadband vibration measurements using a continuously scanning laser vibrometer," *Measurement Science & Technology,* vol. 13, pp. 1574-82, 2002.

[15] A. B. Stanbridge, M. Martarelli, and D. J. Ewins, "Scanning laser Doppler vibrometer applied to impact modal testing," *Shock and Vibration Digest,* vol. 32, p. 35, 2000.

[16] A. B. Stanbridge, M. Martarelli, and D. J. Ewins, "Scanning laser Doppler vibrometer applied to impact modal testing," in *17th International Modal Analysis Conference - IMAC XVII*. vol. 1 Kissimmee, FL, USA: SEM, Bethel, CT, USA, 1999, pp. 986-991.

[17] R. Ribichini, D. Di Maio, A. B. Stanbridge, and D. J. Ewins, "Impact Testing With a Continuously-Scanning LDV," in *26th International Modal Analysis Conference (IMAC XXVI)* Orlando, Florida, 2008.

[18] M. Allen and J. H. Ginsberg, "Floquet Modal Analysis to Detect Cracks in a Rotating Shaft on Anisotropic Supports," in *24th International Modal Analysis Conference (IMAC XXIV)* St. Louis, MO, 2006.

[19] M. S. Allen, "Floquet Experimental Modal Analysis for System Identification of Linear Time-Periodic Systems," in *ASME 2007 International Design Engineering Technical Conference* Las Vegas, NV, 2007.

[20] M. S. Allen, "Frequency-Domain Identification of Linear Time-Periodic Systems using LTI Techniques," *Journal of Computational and Nonlinear Dynamics* vol. 4, 24 Aug. 2009.

[21] R. J. Allemang and D. L. Brown, "A Unified Matrix Polynomial Approach to Modal Identification," *Journal of Sound and Vibration,* vol. 211, pp. 301-322, 1998.
[22] K. Ogata, *Discrete-time control systems*, 2nd Edition ed. Upper Saddle River, New Jersey: Prentice Hall, 1994.
[23] M. W. Sracic and M. S. Allen, "Experimental Investigation of the Effect of Speckle Noise on Continuous Scan Laser Doppler Vibrometer Measurements," in *27th International Modal Analysis Conference (IMAC XXVII)* Orlando, Florida, 2009.
[24] S. D. Stearns, *Digital Signal Processing with Examples in Matlab*. New York: CRC Press, 2003.
[25] P. Guillaume, P. Verboven, S. Vanlanduit, H. Van Der Auweraer, and B. Peeters, "A Poly-Reference Implementation of the Least-Squares Complex Frequency-Domain Estimator," in *International Modal Analysis Conference (IMAC XXI)* Kissimmee, Florida, 2003.
[26] H. Van Der Auweraer, P. Guillaume, P. Verboven, and S. Vanlanduit, "Application of a Fast-Stabilizing Frequency Domain Parameter Estimation Method," *Journal of Dynamic Systems, Measurement, and Control,* vol. 123, pp. 651-658, 2001.
[27] M. S. Allen, "Global and Multi-Input-Multi-Output (MIMO) Extensions of the Algorithm of Mode Isolation (AMI)," in *George W. Woodruff School of Mechanical Engineering* Atlanta, Georgia: Georgia Institute of Technology, 2005, p. 129.
[28] M. S. Allen and J. H. Ginsberg, "Global, Hybrid, MIMO Implementation of the Algorithm of Mode Isolation," in *23rd International Modal Analysis Conference (IMAC XXIII)* Orlando, Florida, 2005.
[29] H. Van Der Auweraer and J. Leuridan, "Multiple Input Orthogonal Polynomial Parameter Estimation," *Mechanical Systems and Signal Processing,* vol. 1, pp. 259-272, 1987.
[30] M. S. Allen and J. H. Ginsberg, "A Global, Single-Input-Multi-Output (SIMO) Implementation of The Algorithm of Mode Isolation and Applications to Analytical and Experimental Data," *Mechanical Systems and Signal Processing,* vol. 20, pp. 1090–1111, 2006.
[31] S. Rothberg, "Numerical simulation of speckle noise in laser vibrometry," *Applied Optics,* vol. 45, pp. 4523-33, 2006.
[32] S. J. Rothberg and B. J. Halkon, "Laser vibrometry meets laser speckle," 1 ed. vol. 5503 Ancona, Italy: SPIE-Int. Soc. Opt. Eng, 2004, pp. 280-91.
[33] T. G. Carne, D. Todd Griffith, and M. E. Casias, "Support conditions for experimental modal analysis," *Sound and Vibration,* vol. 41, pp. 10-16, 2007.
[34] M. Rades and D. J. Ewins, "MIFs and MACs in Modal Analysis," in *20th International Modal Analysis Conference (IMAC-20)* Los Angeles, CA, 2002, pp. 771-778.
[35] M. S. Allen and J. H. Ginsberg, "A linear least-squares version of the algorithm of mode isolation for identifying modal properties. Part II: Application and Assessment," *Journal of the Acoustical Society of America (JASA),* vol. 116, pp. 908-915, 2004.
[36] J. H. Ginsberg and M. S. Allen, "A linear least-squares version of the algorithm of mode isolation for identifying modal properties. Part I: Conceptual development," *Journal of the Acoustical Society of America (JASA),* vol. 116, pp. 900-907, 2004.
[37] M. S. Allen and D. M. Aguilar, "Model Validation of a Bolted Beam Using Spatially Detailed Mode Shapes Measured by Continuous-Scan Laser Doppler Vibrometry," in *50th AIAA/ASME/ASCE/AHS/ASC Structures, Structural Dynamics, and Materials Conference* Palm Springs, California, 2009.